

HYDRATION CHARACTERISTICS OF METAL HYDRIDE FIXED IN RESIN FORM

FUJIO WATANABE, CHIHOMI IKAI AND MASANOBU HASATANI

Department of Chemical Engineering, Nagoya University, Nagoya 464-01

CHISATO MARUMO

Kanebo, Ltd., Osaka 534

Key Words: Material, Hydrogen Storage, Metal Hydride, Resin Form, Absorption Equilibrium, Hydration Rate, Durability

Metal hydride powders were fixed in resin forms of two different shapes, a cylinder and a film. The pressure-composition-temperature (PCT) characteristics and the durability to the hydrating/dehydrating cycles were tested.

The PCT characteristics were found to show a similar trend to that of untreated powders, except for a slight decrease in hydration capacity and a slight increase in the pressure hysteresis. The hydration rate increased with increase in metal hydride content and was not much different from that of powders of samples with a high content of metal hydride. Further, from SEM observation it was confirmed that the metal powders were well fixed in the resin matrix in spite of the breakdown of the powders themselves after several repetitive operations. Little damage was observed to the base resin with repetition.

It is concluded that the metal-hydride fixation tested in this work is applicable as a new functional method with durability.

Introduction

For safe storage of hydrogen gas^{1,3,18)} or for application to a chemical heat pump,^{4,5,12,14,15,20,21,23-25)} interest in metal hydrides has steadily increased in recent years. Metal hydrides are also expected to be usable for the purification of hydrogen,^{3,8)} as fuel cell electrodes,^{11,28)} and in other hydrogen systems.

In the practical use of metal hydrides, however, the breakdown of a metal particle into fine powders is well known as a serious and common problem. During cyclic use of the metal hydride for hydrating and dehydrating, a 10–25% change in molal volume takes place and causes the particle to disintegrate. As a result, heat conduction through the particle bed becomes poorer, and effective removal or supply of the heat accompanying the hydrating and dehydrating reaction becomes difficult. Fine-powders entrainment in the cyclic hydrogen flow is another disadvantage caused by the particle disintegration.

In the last decade, several attempts have been made to relieve the disadvantages caused by particle disintegration. Fixation or envelopment of the metal particle in a micro-capsule^{9,10,21)} or in a thin film^{1,17,22)} are good illustrations. Stabilization by means of amorphous state^{2,17)} is another well-known attempt.

In the present paper, the results of an experimental attempt to fix metal hydride powders in organic resin

forms will be reported. The shapes of the resin forms were a cylinder and a film. For preparation of the resin forms, the technique discussed in the previous papers^{7,26,27)} was employed.

1. Experiment

1.1 Preparation of metal hydride fixed in resin form (MHF)

CaNi₅ powders of which the plateau is situated near the atmospheric pressure under ambient temperature conditions¹⁶⁾ were employed as a metal hydride.

Cylindrical form: The cylindrical type was formed by solidifying a premixture of polyvinyl alcohol, a liquid-state phenol resin, the metal hydride crushed to under 250-mesh fineness, and starch powders in a cylindrical vessel at a temperature of 393 to 453 K. After solidification was confirmed, the starch powder was washed off with water. The preparation process for this sample is fundamentally the same as that for the raw material of structural active carbon production, reported in the previous works.^{26,27)} These samples were 0.025 m in diameter and 0.15 m long and were classified according to metal hydride content as shown for S1 to S3 of **Table 1**. In this production process, the metal hydride content reaches a maximum limit for sample S3.

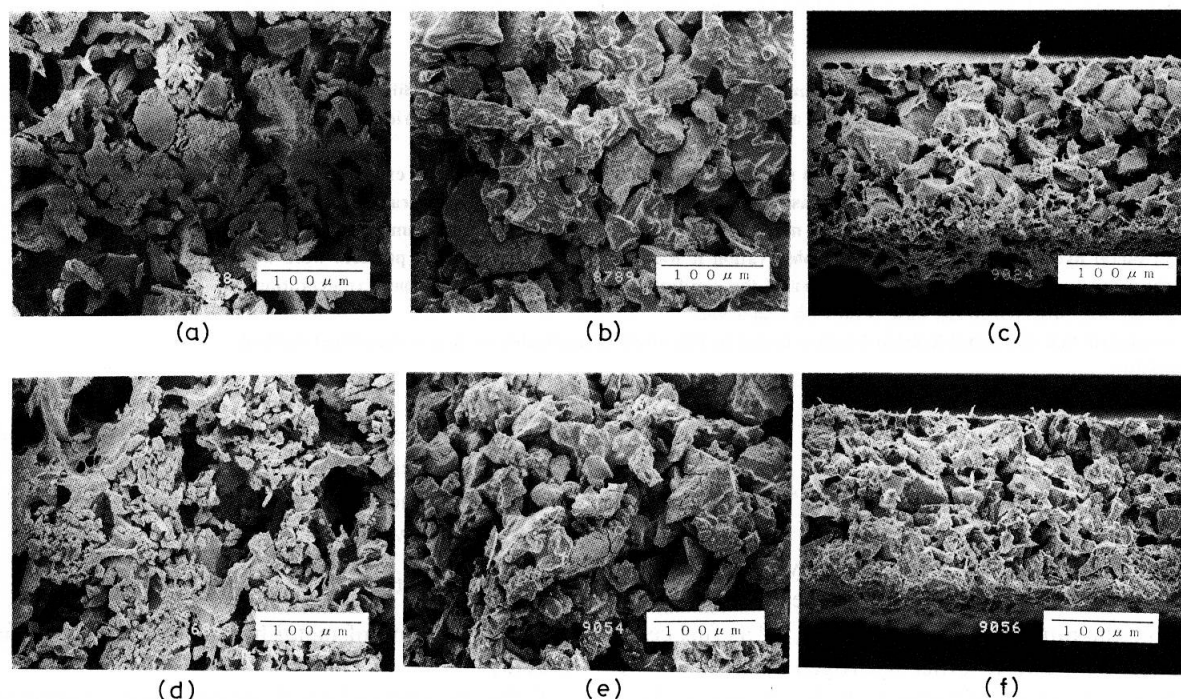
Another (S4) was extruded from a mixture of a fine granular phenol resin, a liquid-state phenol resin and the metal hydride into a cylindrical shape and was then solidified at a temperature of 420 to 430 K.

Figures 1(a) and (b) show scanning electron

* Received January 23, 1991. Correspondence concerning this article should be addressed to M. Hasatani.

Table 1. Physical properties of the MHF

Raw material of matrix	Sample No.	Content of CaNi ₅ [wt%]	Shape	Apparent density [kg·m ⁻³]	Porosity [%]
Polyvinyl alcohol and liquid phenol resin	S1	50	cylindrical	0.411	70
	S2	70	cylindrical	0.600	63
	S3	80	cylindrical	1.01	50
Granular phenol resin and liquid phenol resin	S4	91	cylindrical	1.28	—
Polyvinyl alcohol	S5	85	film	2.37	—
	S6	95	film	2.39	—

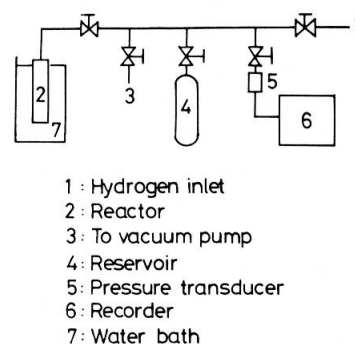
**Fig. 1.** Scanning electron micrographs of MHF samples
(a) S3, (b) S4, (c) S5, (d) S3 after 5 cycles; (e) S4 after 1 cycle; and (f) S5 after 5 cycles

micrographs (SEM) of samples S3 and S4, respectively. Both samples are highly porous, but the metal hydride contained in them is tightly held by the resin matrix.

Film form: This type was prepared from a mixture of polyvinyl alcohol solution and the metal hydride powders extended on a plate. It was solidified at 373 K into a thin film shape of 0.25 mm thickness. It is seen from Table 1 that the metal hydride content for this type of MHF is a little higher than those of the cylindrical type; sample S6 shows the highest value among those tested here. A cross-sectional view of sample S6 in SEM is shown in Fig. 1(c). In this type of MHF the metal hydride is also fixed well in the resin matrix, as if the metal particles were pasted with the resin.

1.2 Measurements of the characteristics of hydrogen absorption

As hydrogen absorption characteristics of the

**Fig. 2.** Schematic diagram of apparatus for measuring PCT characteristics

MHF, the pressure-composition-temperature (PCT) curve and the hydration rates were measured by using the apparatus shown in Fig. 2. The apparatus is designed to withstand a pressure of 30 kPa. It includes

a hydrogen inlet (1); a reactor (2) with an inner volume of 143 cm³ placed in a temperature controller with water circulator actuated at a given constant temperature; a vacuum system (3); a hydrogen reservoir (4); and a pressure transducer (5). A sintered metal filter with a pore size of 0.5 μ was fixed at the reactor inlet to protect the dispersion of particles. The equilibrium pressure was measured with a pressure transducer. Hydrogen gas of 99.995% purity was provided for this experiment.

In the measurements of the PCT curves and the hydriding kinetics, about 15 g of MHF was loaded in the reactor. The MHF was activated by repeating the following procedures four times prior to the measurements; the sample was evacuated at 373 K up to 10⁻³ torr for 24 hours, and then hydrogen gas was introduced in the reactor at about 2.0 MPa.

After completion of the activation procedures was confirmed, the hydration and dehydration experiments were carried out under a hydration starting pressure of 10⁻³ torr in the same way as in the previous studies.^{6,19} In these experiments, the time required to reach equilibrium was about 6 hours, but 24 hours was spent in every run for confirmation.

1.3 Observation of structure change

Hardly any structure change due to the hydriding/dehydriding cycles was observed by SEM observation or by direct observations.

2. Results and Discussion

2.1 PCT curve and structure change

The PCT curves measured in the first cycle of hydration/dehydration for the MHF are shown in **Figs. 3 and 4** in comparison with those of the untreated metal hydride. The maximum amount of hydrogen absorbed ((*H/M*)_{max}), the plateau pressure in the hydration (*P*_a) and the dehydration (*P*_b) found from these figures for each sample are listed in **Table 2** together with the hysteresis factor (*H_f*) defined by the following equation.

$$H_f = \ln(P_a/P_b) \quad (1)$$

On comparing the samples prepared and the untreated metal hydride, several features can be observed from Figs. 3, 4 and Table 2.

1) The shape and the slope of the plateau in the PCT curve of the MHF are the same as those of the untreated metal hydride.

2) In the cylindrical and film forms, the (*H/M*)_{max} values are limited to 81% and 91% of that in the untreated metal hydride on average, respectively.

3) For all samples, both plateau pressures, *P*_a and *P*_b, are a little lower than that for the untreated metal hydride, and the *H_f*-values are 1.4 to 2.2 times larger.

Figure 5 shows the influence of the number of cycles on the PCT curve of the MHF. Only a small difference

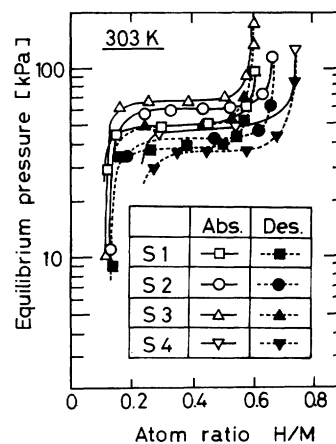


Fig. 3. PCT curves of samples S1 to S4

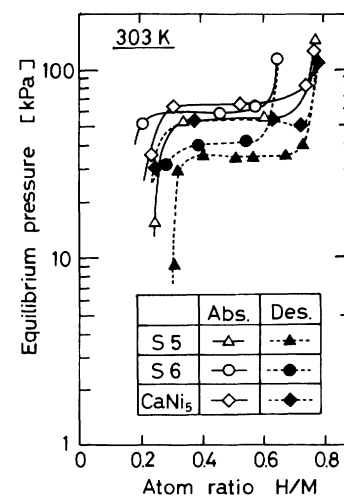


Fig. 4. PCT curves of samples S5, S6 and CaNi₅

Table 2. Absorption and desorption characteristics for the MHF produced

Sample	(<i>H/M</i>) _{max}	<i>P</i> _a [kPa]	<i>P</i> _b [kPa]	<i>H_f</i> (= ln <i>P</i> _a / <i>P</i> _b) [—]
CaNi ₅	0.78	65	54	0.19
S1	0.60	53	38	0.33
S2	0.67	59	43	0.26
S3	0.60	66	50	0.26
S4	0.75	48	36	0.24
S5	0.78	55	35	0.45
S6	0.64	60	42	0.41

is seen between the 1st at 5th cycles.

It was found from the structural observations that there is almost no trace of the damage to the resin matrix of the MHF. Segregation of the metal hydride particles from the MHF phase was slight and the metal hydride particles were observed to be firmly fixed in the resin matrix even though disintegration of the powders themselves took place during the hydriding/dehydriding cycles. **Fig. 1(d) to (f)** show comparisons of SEM photographs of the MHF after

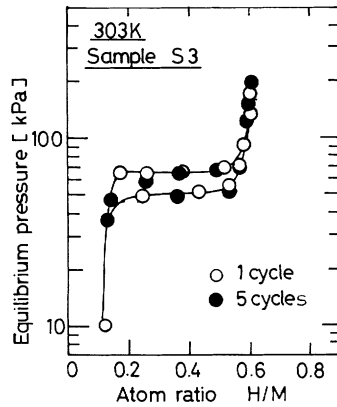


Fig. 5. Influence of hydriding/dehydriding cycles on PCT characteristics

cycle use. The reduction in diameter of the metal hydride particles during the cyclic repetitions, measured from SEM results, is shown in Fig 6.

The above results indicate that the total hydrogen absorption capacity of the MHF produced is lower than that of the untreated metal hydride, as shown in the trends of the $(H/M)_{\max}$ - and the H_f -values in the PCT curves. However, the reduction in total capacity is not serious, and it can be suggested that the fixation of hydriding alloy particles in the resin form offers a practical solution to the problem of disintegration of the metal hydride accompanying the hydriding/dehydriding cycle.

2.2 Hydration rate

Examples of the hydration rates measured at 303K by a constant-volume method for the untreated metal hydride and each sample are shown in Figs. 7 and 8, where $(H/M)_0$ is the equilibrium atom ratio for each sample at the initial pressure (P_0). In these experiments, the initial weight of CaNi_5 contained in the MHF was adjusted to be equal to that in the untreated metal hydride.

Figure 7 shows that the time changes of $(H/M)/(H/M)_0$ for each sample are affected by P_0 and in this experimental region the hydration rates are apparently in proportion to P_0 . Therefore, comparing the hydration rates with the results at $P_0=220$ kPa, the following is learned from Fig. 8. The time required for reaching 90% of $(H/M)_0$ is more than 3 h, 1.6 h, 1.4 h and 1.2 h for samples S1 to S4, respectively. Also, it is about 0.9 h for S5, S6 and bare CaNi_5 , but the curves of $(H/M)/(H/M)_0$ for S5 and S6 are a little lower than that for bare CaNi_5 in the early period. In addition to these results, it was seen in this experimental region that the curves of $(H/M)/(H/M)_0$ after several repetitive uses are about the same as those in the first hydration.

It is seemed from these results that the hydration rates for all the MHF prepared are less than that for the untreated metal hydride, but they increase with

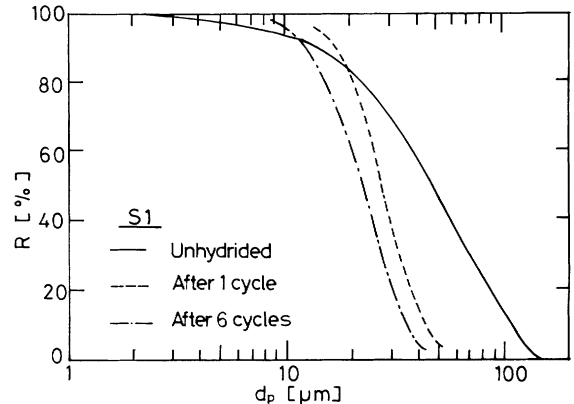


Fig. 6. Change of CaNi_5 particle size for cyclic uses

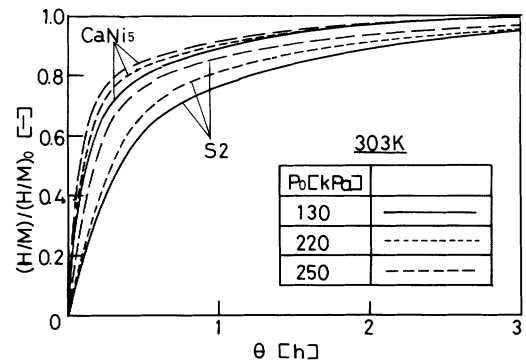


Fig. 7. Influence of initial pressure on hydration rate for MHF sample S2 and CaNi_5

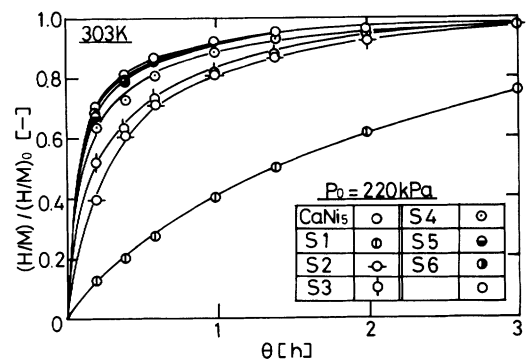


Fig. 8. Hydration rates for MHF sample S1 to S6

increase in metal hydride content. As for the hydration rate, the ability for the MHFs prepared in this work are lower than that for the microencapsulation metal hydride by H. Ishikawa *et al.*¹⁰⁾ However, in particular the hydration rates for the film-type MHFs and for the cylindrical-type MHF containing a high level of metal hydride, such as sample S4, are not much different from that for the untreated metal hydride. Consequently, it is thought that these MHFs are usable as a new type of hydrogen absorbent.

Conclusion

With the aim of improving the durability of metal

hydrides, fixation of metal hydride powders in organic resin forms (MHF) of two different shapes, cylindrical and film forms, was attempted experimentally. For each sample prepared the hydrogen absorption characteristics, the effects of cyclic hydriding/dehydriding use on durability, and the hydration rates were investigated.

1) The hydrogen absorption equilibrium characteristics of the MHF are similar to those of untreated powders, except for a slight decrease in hydration capacity and a slight increase in the pressure hysteresis.

2) Metal powders are well fixed in the resin matrix in spite of the breakdown of the powders themselves after several repetitive uses. Little damage to the base resin with repetition was observed.

3) The hydration rate in the MHF increases with increase of metal hydride content, and are the closer to that of the untreated metal hydride for the film-type MHFs and for the cylindrical-type MHFs containing a high level of metal hydride.

Therefore, it was demonstrated that the MHFs prepared in this work are usable as a new type of hydrogen absorbent with durability.

Acknowledgment

This work was partially supported by a Grant-in-Aid for Science Research, the Ministry of Education, Science and Culture, Japan (Grant No. 62850160).

Nomenclature

d_p	= particle diameter	[μm]
H	= number of hydrogen atoms	
H_f	= hysteresis factor	[—]
M	= number of metal hydride atoms	
P_0	= initial pressure	[kPa]
P_a	= plateau pressure in hydration	[kPa]
P_b	= plateau pressure in dehydration	[kPa]
R	= cumulative plus sieve percentage	[%]
θ	= time	[h]

Literature Cited

1) Adachi, G., H. Nagai and J. Shiokawa: *J. Less-Common Met.*,

- 97, 9 (1984).
- 2) Aoki, K. and K. Matsumoto: *Nippon Kinzoku Gakkai Kaiho*, **23**, 818 (1984).
- 3) Block, F. R. and H. J. Bahs: *J. Less-Common Met.*, **104**, 223 (1984).
- 4) Lynch, F. E.: *J. Less-Common Met.*, **74**, 411 (1980).
- 5) Fukai, Y.: *Ooyo Butsuri*, **48**, 1035 (1979).
- 6) Gruen, D. M., M. H. Mendelsohn and I. Sheft: *Solar Energy*, **21**, 153 (1982).
- 7) Hasatani, M., F. Watanabe and C. Marumo: *Kagaku Kogaku Ronbunshu*, **14**, 79 (1988).
- 8) Hirata, T.: *J. Less-Common Met.*, **107**, 23 (1985).
- 9) Ishikawa, H., K. Oguro, A. Kato, H. Suzuki and E. Ishii: *J. Less-Common Met.*, **107**, 105 (1985).
- 10) Ishikawa, H., K. Oguro, A. Kato and H. Suzuki: *Kagaku Kogaku*, **50**, 256 (1986).
- 11) Iwakura, C., T. Asaoka, T. Sakai, H. Ishikawa and K. Oguro: *Denki Kagaku*, **53**, 722 (1985).
- 12) Iwasaki, M., S. Kawai, R. Ishikawa and Y. Komazaki: *Chem. Eng.*, **31**, 905 (1986).
- 13) Ono, S.: *Denki Kagaku*, **44**, 818 (1976).
- 14) Ono, S.: *Denki Kagaku*, **46**, 388 (1978).
- 15) Ono, S. and Y. Oosumi: *Ceramics*, **14**, 339 (1979).
- 16) Oosumi, Y.: "Kinzoku Suisokabutsu", p. 41, Kagakukogyosha, Tokyo (1983).
- 17) Oosumi, Y.: *Chemical Eng.* **30**, 616 (1985).
- 18) Nakajima, M.: *Kagaku Kogaku*, **49**, 379 (1985).
- 19) Nomura, I. and S. Ono: *Kagaku Kogaku*, **49**, 630 (1985).
- 20) Northrup, Jr. C. J. M. and A. A. Heckes: *J. Less-Common Met.*, **74**, 419 (1980).
- 21) Ron, M.: *J. Less-Common Met.*, **104**, 259 (1984).
- 22) Sakaguchi, H., N. Taniguchi, H. Seri, K. Adachi and J. Shiokawa: *Nippon Kagaku Kaishi*, **1987**, 1875 (1987).
- 23) Sheft, I., D. M. Gruen and G. M. Lamich: *J. Less-Common Met.*, **74**, 401 (1980).
- 24) Suda, S.: *Chem. Eng.*, **28**, 349 (1983).
- 25) Suda, S.: *J. Less-Common Met.*, **104**, 211 (1984).
- 26) Watanabe, F., N. Kamiya and M. Hasatani: *Kagaku Kogaku Ronbunshu*, **10**, 574 (1984).
- 27) Watanabe, F., M. Hasatani, N. Kamiya, T. Kato and C. Marumo: *Kagaku Kogaku Ronbunshu*, **11**, 481 (1985).
- 28) Yayama, H., R. Tomokiyo and K. Hirakawa: *Ooyo Butsuri*, **56**, 216 (1987).

(Presented at the 51 st Annual Meeting of the Society of Chemical Engineers, at Osaka, March, 1986 and at the 20th Autumn Meeting of the Society of Chemical Engineers, at Himeji, October, 1987)